Materials Science-Poland, 32(4), 2014, pp. 719-728
http://www.materialsscience.pwr.wroc.pl/
DOI: 10.2478/s13536-014-0254-5

VERSITA

FP-LMTO study of structural, electronic, thermodynamic and optical properties of $Mg_xCd_{1-x}Se$ alloys

D. BENSAID[1], M. AMERI[1*], M. DIN EL HANANI[1], Y. AZAZ[1], D. BENDOUMA[2], Y. AL-DOURI[3], I. AMERI[4]

[1]Laboratory of Physical Chemistry of Advanced Materials, University of Djillali Liabes, BP 89, Sidi-Bel-Abbes 22000, Algeria

[2]Physics Department, Faculty of Sciences, Dr. Moulay Tahar University of Saïda, 20000 Saïda, Algeria

[3]Institute of Nano Electronic Engineering, University Malaysia Perlis, 01000 Kangar, Perlis, Malaysia

[4]Djillali Liabes University, Faculty of Exact Sciences, Department of Physics, PO Box 089, Sidi Bel Abbes, 22000, Algeria

Structural, electronic and optical properties of $Mg_xCd_{1-x}Se$ $(0 \leqslant x \leqslant 1)$ are calculated for the first time using density functional theory. Our results show that these properties are strongly dependent on molar fraction of particular components – x. The bond between Cd and Se is partially covalent and the covalent nature of the bond decreases as the concentration of Mg increases from 0 % to 100 %. It is found that $Mg_xCd_{1-x}Se$ has a direct band gap in the entire range of x and the band gap of the alloy increases from 0.43 to 2.46 eV with the increase in Mg concentration. Frequency dependent dielectric constants $\varepsilon_1(\omega), \varepsilon_2(\omega)$ refractive index $n(\omega)$ are also calculated and discussed in detail. The peak value of refractive indices shifts to higher energy regions with the increase in Mg. The larger value of the extraordinary refractive index confirms that the material is a positive birefringence crystal. The present comprehensive theoretical study of the optoelectronic properties of the material predicts that it can be effectively used in optoelectronic applications in the wide range of spectra: IR, visible and UV. In addition, we have also predicted the heat capacities (C_V), the entropy (S), the internal energy (U) and the Helmholtz free energy (F) of $Mg_xCd_{1-x}Se$ ternary alloys.

Keywords: *structural properties; electronic and optical properties; thermodynamic properties; FP-LMTO method; ternary alloy*

1. Introduction

Mg-based II – VI semiconductors have recently attracted much attention because of their potential applications in the field of blue-green light sources and other optoelectronic devices (i.e. construction of blue-green laser diode operating at room temperature (RT)) [1]. These alloys have the possibility of tuning the band gap and lattice constants by varying the Mg concentration. $Mg_xCd_{1-x}Se$ alloys have attracted great attention because they are promising for the fabrication of full-color visible optical devices due to a large difference in the energy gaps Eg of the binary constituents (CdSe, Eg = 1.74 eV; MgSe, Eg = 4.0 eV) [2] To date, only few papers have been reported on the recombination processes in $Mg_xCd_{1-x}Se$ crystals and the fabrication of green-light-emitting structures using n-CdSe and p-ZnTe regions separated by a graded $Mg_xCd_{1-x}Se$ injection region [1–8].

In the present theoretical work, the band gap of zinc-blende CdSe has been varied systematically by alloying with Mg. In order to investigate optoelectronic nature of these alloys, their structural, electronic and optical properties are calculated. All calculations are based on density functional full-potential linear muffin-tin orbital (FP-LMTO) method with Perdew-Wang generalized gradient approximation (GGA).

*E-mail: lttnsameri@yahoo.fr

2. Method of calculations

The calculations reported here were carried out using the *ab initio* full-potential linear muffin-tin orbital (FP-LMTO) method [9–12] as implemented in the Lmtart code [13]. The exchange and correlation potential was calculated using the generalized gradient approximation (GGA) [14]. The FP-LMTO is an improved method compared to previous LMTO techniques, and treats muffin-tin spheres and interstitial regions on the same footing, leading to improvements in the precision of the eigenvalues. At the same time, the FP-LMTO method, in which the space is divided into interstitial regions (IR) and non-overlapping muffin-tin spheres (MTS) surrounding the atomic sites, uses a more complete basis than its predecessors. In the IR regions, the basis set consists of plane waves. Inside the MT spheres, the basis sets is described by radial solutions of one particle Schrödinger equation (at fixed energy) and their energy derivatives multiplied by spherical harmonics. The charge density and the potential are represented inside the MTS by spherical harmonics up to $l_{max} = 6$. The integrals over the Brillouin zone are performed up to 35 special k-points for binary compounds and 27 special k-points for the alloys in the irreducible Brillouin zone (IBZ) using Blochl's modified tetrahedron method [15]. The self-consistent calculations are considered to be converged when the total energy of the system is stabled within 10^{-6} Ry. In order to avoid the overlap of atomic spheres, the MTS radius for each atomic position is taken to be different for each composition. We point out that the use of the full-potential calculation ensures that the calculation is not completely independent of the choice of sphere radii.

Structural properties of $Mg_xCd_{1-x}Se$ are calculated using Murnaghan's equation of state [16]:

$$E(V) = E_0 + \frac{B_0 V}{B'_0}\left(\frac{(V_0/V)^{B'_0}}{B'_0 - 1} + 1\right) - \frac{B_0 V_0}{B'_0 - 1} \quad (1)$$

where E_0 is the total energy of the supercell, V_0 is the unit volume, B_0 is the bulk modulus at zero pressure and B'_0 is the derivative of bulk modulus with respect to pressure.

Optical properties of $Mg_xCd_{1-x}Se$ are calculated using a fine k mesh of 1500 points. The dielectric constant of a crystal depends on the electronic band structure and its investigation by optical spectroscopy is a powerful tool in the determination of the overall optical behavior. It can be divided into two parts, real and imaginary:

$$\varepsilon(\omega) = \varepsilon_1(\omega) + i\varepsilon_2(\omega) \quad (2)$$

The imaginary part of the complex dielectric constant $\varepsilon_2(\omega)$ in cubic symmetry compounds can be calculated by the following relation [17, 18]:

$$\varepsilon_2(\omega) = \frac{8}{2\pi\omega^2}\sum_{nn}\int |pnn'(k)|^2 \frac{dSk}{\nabla\omega nn'(k)} \quad (3)$$

while $\varepsilon_1(\omega)$ is used to calculate the real part of the complex dielectric-constant:

$$\varepsilon_1(\omega) = 1 + \frac{2}{\pi}p\int_0^\infty \frac{\omega'\varepsilon_2(\omega')}{\omega'^2 - \omega'^2}d\omega' \quad (4)$$

Refractive index is calculated in terms of real and imaginary parts of dielectric constant by the following relation:

$$n(\omega) = \frac{1}{\sqrt{2}}[\{\varepsilon_1(\omega)^2 + \varepsilon_2(\omega)^2\}^{\frac{1}{2}} + \varepsilon_1(\omega)]^{\frac{1}{2}} \quad (5)$$

3. Results and discussion

3.1. The crystal structure

The starting binary compound for all the ternary alloys, i.e. CdSe has been modeled in the B3 structure and the alloy's unit cell has then been obtained for the compositions x = 0.25, 0.50, 0.75, and 1.0 by replacing one, two, three, and four Cd atoms, respectively, from the CdSe lattice by Mg atoms for obtaining the $Mg_xCd_{1-x}Se$ alloys. The crystal structure of CdSe and MgSe is zinc-blende with space group $F\bar{4}3m$ (no. 216). We performed the structural optimization by minimizing the total energy with respect to the cell parameters and also the atomic positions.

The total energies calculated as a function of unit cell volume were fitted to the Murnaghan's equation of state. The corresponding equilibrium lattice constants and bulk moduli both for binary

compounds and their alloys are given in Table 1. Considering the general trend that GGA usually overestimates the lattice parameters [19], our GGA results of binary compounds are in reasonable agreement with the experimental and other calculated values. Usually, in the treatment of alloys, it is assumed that the atoms are located at the ideal lattice sites and the lattice constant varies linearly with composition x according to the so-called Vegard's law [20]. However, violation of this linear law has been reported in semiconductor alloys both experimentally [21, 22] and theoretically [23, 24]. We show in Fig. 1 the effect of Mg substitutional impurities on the lattice parameters for both the GGA and VCA approaches. We can note no deviation from Vegard's law for x concentration in the range of 0 to 1. An analytical relation for the compositional dependence of the Mg lattice parameter is given by the quadratic fit:

$$a_x = 6.259 - 0.251x + 0.001x^2 \qquad (6)$$

Fig. 1 and 2 show the variation of the calculated equilibrium lattice constant and bulk modulus as a function of concentration x for the $Mg_xCd_{1-x}Se$ alloy. The obtained results for the composition dependence of the calculated equilibrium lattice parameter almost follow Vegard's law [20]. In going from CdSe to MgSe, when the Mg-content increases, the values of the lattice parameters of the $Mg_xCd_{1-x}Se$ alloy decrease. This is due to the fact that the size of Mg atom is smaller than that of Cd atom. On the opposite side, one can see from Fig. 2 that the value of the bulk modulus increases as the Mg concentration increases.

3.2. The electronic properties

The calculated band structure for $Mg_xCd_{1-x}Se$ ($0 \leqslant x \leqslant 1$) is presented in Fig. 2. It is clear from the figure that $Mg_xCd_{1-x}Se$ ($0 \leqslant x \leqslant 1$) is a direct band gap material. The substitution of Mg does not affect the indirect band gap nature of the compound but increases the gap, which is clear from Fig. 2d. The direct band gap also increases from 0.43 to 2.46 eV with the increase in Mg concentration. It is obvious from the data presented in Table 2 that our calculated values for the band gaps of CdSe and

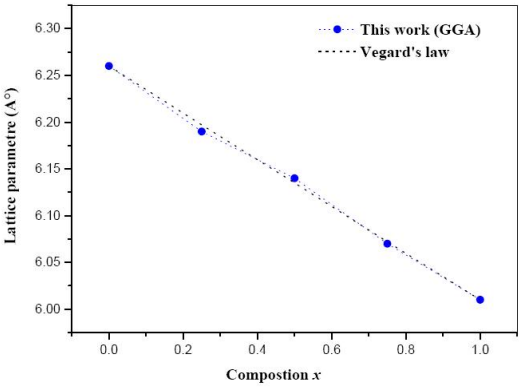

Fig. 1. Variation in lattice constant B of $Mg_xCd_{1-x}Se$ as a function of composition x.

MgSe are closer to theoretical results. The reason for our better results is the use of effective Perdew-Wang potential in the GGA scheme [14], and high number of k-points (3500). DFT always underestimates the band gaps [33]; to avoid this problem we calculated the direct band gap bowing coefficients using the following relation [34, 35]:

$$E_g^{A_xB_{1-x}C} = xE_g^{AC} + (1-x)E_g^{BC} - x(1-x)b \qquad (7)$$

where $E_g^{A_xB_{1-x}c}$, E_g^{AC} and E_g^{BC} are the energy band gaps of the ternary alloys $A_xB_{1-x}c$ and its binary parents AC and BC, respectively. The curvature b is commonly known as the band gap bowing parameter. For $Cd_{1-x}Mg_xSe$, we have taken into account the composition linear dependence on b. The results obey the following variations:

$$Cd_{1-x}Mg_xSe \rightarrow \begin{matrix} E_{\Gamma-\Gamma} = 0.438 + 1.833x + 0.194x^2 \\ E_{\Gamma-X} = 1.807 + 1.142x - 0.994x^2 \end{matrix} \qquad (8)$$

The origin of the band structures presented in Fig. 2 can be understood by the corresponding density of states [36]. It is clear from the results that the conduction band is mainly composed of Mg-3s state for all ternary alloys. Fig. 2 (a – c) shows that the lower part of the valence band is composed of Cd-4d and the upper part is mainly dominated by Se-4p state. The variation in the band gap of $Mg_xCd_{1-x}Se$ ($0 \leqslant x \leqslant 1$) provides promising results of the use of the compound in optoelectronic devices working in visible to ultraviolet region. Depending on the need and requirement of

Table 1. Lattice constants a and bulk modulus B of $Mg_xCd_{1-x}Se$ compared with experimental results, Vegard's law and other theoretical calculations.

	Lattice constant a (Å)				Bulk modulus B (GPa)[B′]		
x	This work	Exp	Vegard's law	Other calc.	This work	Exp	Other calc.
0	6.26	6.052[a]		6.025[b]	42.92 [4.18]	55[c]	54[d]
0.25	6.19		6.197		44.4 [3.94]		
0.5	6.14		6.135		43.51 [4.33]		
0.75	6.07		6.072		45.43 [4.07]		
1	6.01	5.89[e]		5.70[f], 5.89[g]	62.16 [4.50]		48[4.27][g], 50[4.02][h]
				5.88[h], 5.92[i], 5.893[j]			49[3.75][i], 51[4.01][j]

[a][23], [b][24], [c][25], [d][26], [e][27], [f][28], [g][29], [h][30], [i][31], [j][32].

Table 2. Fundamental direct and indirect band gaps of $Mg_xCd_{1-x}Se$ compared with the experimental and other calculations.

	Direct energy band gap, $E_g^{\Gamma-\Gamma}$			Indirect energy band gap, $E_g^{\Gamma-x}$		
x	This work	Exp	Other calc.	This work	Exp	Other calc.
0	0.43	1.75[a]	0.34[b] ,0.26[c]	2.00	5.4[d]	4.37[e], 3.82[f]
0.25	0.94	2.22[a]		1.65		
0.5	1.36	2.7[g] [x = 0.44]		2.12		
$Zn_{0.5}Mg_{0.5}Se$		3.39[a]				
0.75	1.95			2.50		
1	2.46	3.59[h] [297K]	3.67[i] 2.56 [j]	1.76		3.2[e]

[a][37], [b][24], [c][25], [d][38], [e][39], [f][40], [g][41], [h][42], [i][43], [j][44].

a particular application, any desired band gap between 0.43 and 2.46 eV can be achieved.

The physical origins of the bowing parameter were investigated following the approach of Zunger and co-workers [45], which decomposes into three contributions:

$$b = b_{VD} + b_{CE} + b_{SR} \tag{9}$$

The corresponding contribution to the total gap bowing parameter b_{VD} represents the relative response of the band structure of the binary compounds AB and AC to hydrostatic pressure, which here arises from the change in their individual equilibrium lattice constants relative to the alloy value a = a(x) (from Vegard's rule). The second contribution, the charge-exchange (CE) contribution b_{CE}, reflects a charge transfer effect, which is due to the different (averaged) bonding behavior at the lattice constant a. The final step represent changes due to the structural relaxation (SR) in passing from the unrelaxed to the relaxed alloy by b_{SR}. The calculated bowing parameter contributions of the direct band gap are presented in Table 3. It is clearly seen that the calculated from the polynomial function bowing parameter within GGA is very close to the results obtained by the Zunger approach [45, 46]. In the case of $Mg_xCd_{1-x}Se$, the different contributions to the direct bowing parameter are found to be very small. The main contribution to the bowing parameter is raised from the structural relaxation effect and the relative response. This can be clearly attributed to the large iconicity mismatch of the binary compounds MgSe ($f_i = 0.79$), and CdSe ($f_i = 0.13$), and the weak mismatch of the lattice constants of the corresponding binary compounds, respectively.

3.3. The optical properties

The calculated imaginary part of the dielectric constant for $Mg_xCd_{1-x}Se$ ($0 \leqslant x \leqslant 1$) in the

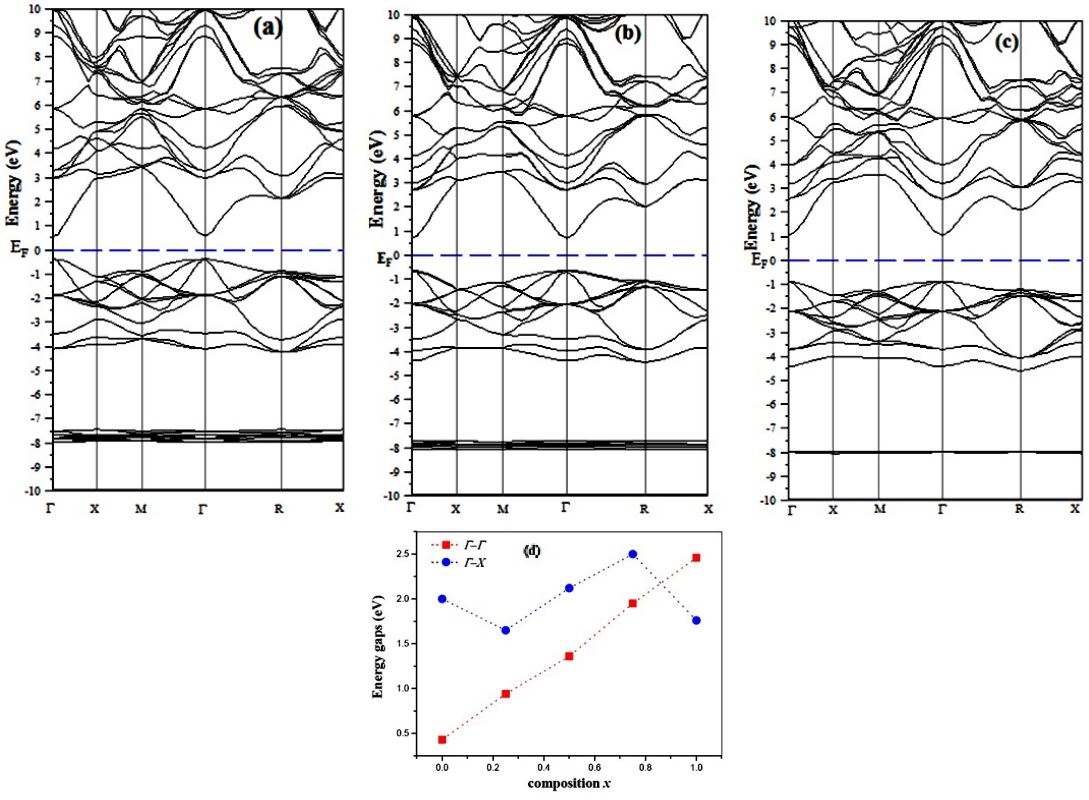

Fig. 2. Calculated band structures of (a) $Cd_{0.75}Mg_{0.25}Se$, (b) $Cd_{0.5}Mg_{0.5}Se$, (c) $Cd_{0.25}Mg_{0.75}Se$ and (d) band gap as a function of x.

Table 3. Decomposition of optical bowing into volume deformation (VD), charge exchange (CE), and structural relaxation (SR) contributions compared with that obtained by a quadratic fit (all values are in eV).

System	Using Zunger approach	From polynomial function fit	Other calc.
$Mg_xCd_{1-x}Se$			
b_{VD}	1.46		
b_{CE}	−2.52		
b_{SR}	1.40		
b	0.34	0.19	0.2[a] [x ⩽ 0.32]

[a][47]

Table 4. Refractive index, optical dielectric constant of $Mg_xCd_{1-x}Se$ alloys for different compositions x.

	Refractive index n			Optical dielectric constant ε		
x	This work	Exp	Other calc.	This work	Exp	Other calc.
0	2.02	2.64[a]	2.49[b] 2.5[c]	4.11	5.2[d]	5.05[e] 4.89[f]
0.25	1.89			3.59		
0.5	1.82			3.33		
0.75	1.74			3.03		
1	1.4		2.03[b]	1.98	7.65[g]	3.8[g]

[a][48], [b][49], [c][50], [d][51], [e][52], [f][53], [g][54].

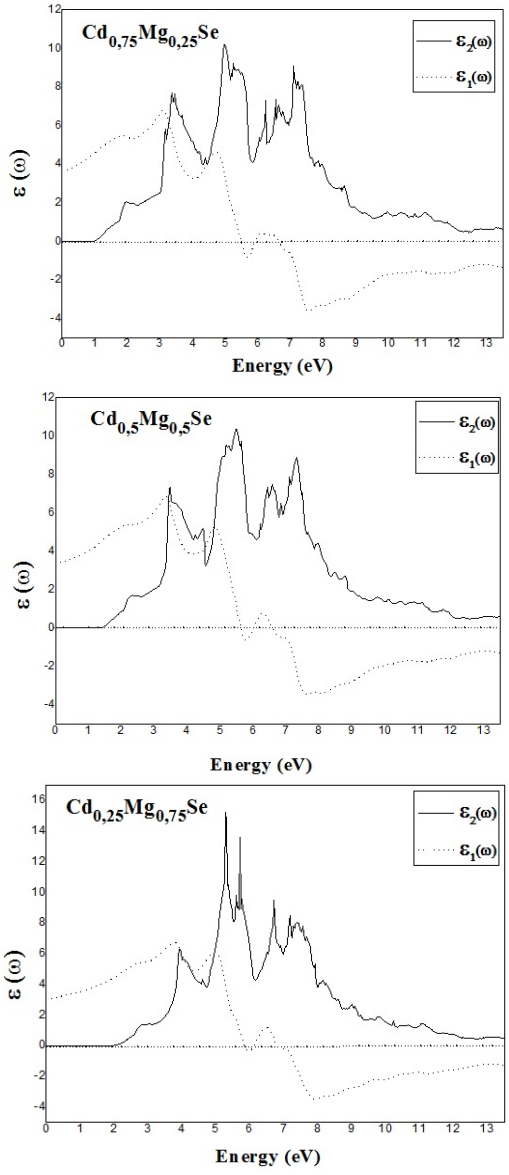

Fig. 3. Frequency dependent imaginary part and real part of dielectric functions/constants of $Mg_xCd_{1-x}Se$.

energy range of 0 to 13.5 eV is shown in Fig. 3. It is clear from the figure that for x = 0, 0.25, 0.50, 0.75 and 1.0 the critical points in the imaginary part of the dielectric function occur at about 0.43, 0.81, 1.36, 1.95 and 1.11 eV, respectively. These points are closely related to the direct band gaps, $E_g^{\Gamma-\Gamma}$; 0.43, 0.94, 1.36, 1.95 and 2.46 eV of $Mg_xCd_{1-x}Se$ for the corresponding values of x = 0, 0.25, 0.50, 0.75 and 1. The calculated real parts of the complex dielectric constant $\varepsilon_1(\omega)$ for $Mg_xCd_{1-x}Se$ are presented in Fig. 3. It is clear from the figure that the static dielectric constant, $\varepsilon_1(\omega)$, is strongly dependent on the band gap of the compound. The calculated values of $\varepsilon_1(\omega)$ for $Mg_xCd_{1-x}Se$ at x = 0, 0.25, 0.50, 0.75 and 1.0 are 4.13, 3.55, 3.32, 3.02 and 4.28 for corresponding direct band gaps 2.00, 1.65, 2.12, 2.50 and 1.76 eV, respectively. These data explain that the smaller energy gap yields larger $\varepsilon_1(0)$ value. This inverse relation of $\varepsilon_1(\omega)$ with the band gap can be explained by the Penn model [40]:

$$\varepsilon_1(0) \approx 1 + (\hbar\omega_p/E_g)^2 \tag{10}$$

The calculated values of the optical dielectric constant $\varepsilon(\omega)$ and refractive index $n(\omega)$, are listed in Table 4. Comparison with the available data has been made where possible. As compared with other calculations, it seems that the values of $n(\omega)$ obtained from FP-LMTO method for the end-point compounds (i.e. CdSe and MgSe) are in good agreement with theoretical results together with the refractive index $n(\omega) = \sqrt{\varepsilon}$ at zero pressure. Note that ε is obtained from the zero-frequency limit of $\varepsilon_1(\omega)$, and it corresponds to the electronic part of the static dielectric constant of the material, a parameter of fundamental importance in many aspects of materials properties. It is clear from Fig. 4 that the refractive index of the material decreases with the increase in the Mg concentration. Fig. 4 shows the variation of the computed static optical dielectric constant and static refractive index versus composition of $Mg_xCd_{1-x}Se$ alloys. The computed static optical dielectric constant and static refractive index versus composition were fitted by polynomial equation. The results are summarized as follows:

$$Mg_xCd_{1-x}Se \rightarrow \begin{cases} \varepsilon_0 = 4.0148 + 0.6708x + 1.2571x^2 \\ n_0 = 1.9905 + 0.0645x - 0.4919x^2 \end{cases} \tag{11}$$

3.4. Thermodynamic properties

In this study, the quasi-harmonic Debye model [54–58] is used to obtain the thermodynamic

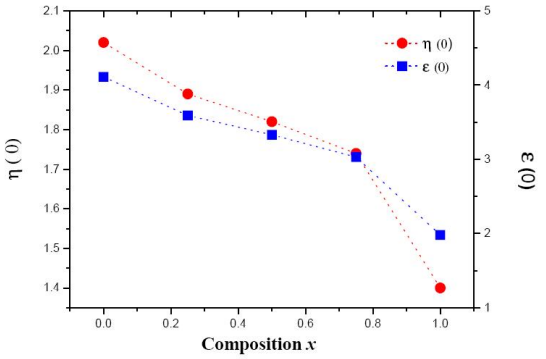

Fig. 4. Computed static optical dielectric constant and static refractive index as a function of composition for $Mg_xCd_{1-x}Se$.

properties of $Mg_xCd_{1-x}Se$. The non-equilibrium Gibbs function G*(V, P, T) is expressed as:

$$G^*(V,P,T) = E(V) + PV + A_{vib}[\Theta(V);T] \quad (12)$$

Here, E(V) is the total energy per unit cell for $Mg_xCd_{1-x}Se$, PV is the constant hydrostatic pressure condition, Θ(V) is the Debye temperature, and the vibrational Helmholtz free energy A_{vib} can be written as [56, 57]:

$$A_{vib}(\Theta;T) = nkT\left[\frac{9}{8}\frac{\Theta}{T} + 3\ln(1-e^{-\Theta/T}) - D\left(\frac{\Theta}{T}\right)\right] \quad (13)$$

where n is the number of atoms per formula unit, D(Θ/T) is the Debye integral. For an isotropic solid [59]:

$$\Theta = \frac{\hbar}{K}[6\pi^2 V^{1/2} n]^{1/3} f(\sigma)\sqrt{\frac{B_S}{M}} \quad (14)$$

where M is the molecular mass per unit cell and B_S is the adiabatic bulk modulus. The non-equilibrium Gibbs function G*(V, P, T) as a function of (V; P, T) can be minimized with respect to volume V as:

$$\left[\frac{\delta G^*(V,P,T)}{\delta V}\right]_{P,T} = 0 \quad (15)$$

The thermal properties, such as internal energies U, entropy S, heat capacity at constant volume C_V, and thermal expansion α are taken as:

$$U = nkT\left[\frac{9}{8}\frac{\Theta}{T} + 3D\left(\frac{\Theta}{T}\right)\right] \quad (16)$$

$$S = nK\left[4D\left(\frac{\Theta}{T}\right) - 3\ln\left(1-e^{-\frac{\Theta}{T}}\right)\right] \quad (17)$$

$$C_V = 3nk\left[4D\left(\frac{\Theta}{T}\right) - \frac{3\Theta/T}{e^{R/T-1}}\right] \quad (18)$$

$$\alpha = \frac{\gamma c_v}{B_T V} \quad (19)$$

Here, γ is the Grüneissen parameter, which is given by the following equation [54]:

$$\gamma = -\left(\frac{d\ln\Theta(V)}{d\ln V}\right) \quad (20)$$

The variation of the entropy (S) and the internal energy (U) versus temperature (T) of the compounds is shown in Fig. 5 (using GGA). It can be seen from this figure that when the temperature increases, the values of the internal energy (U) for $Mg_xCd_{1-x}Se$ increase gradually. Also, the value of U at zero temperature, that represent the zero point motion, is 4.36 kJ/mol·cell and 13.370 kJ/mol·cell for CdSe and MgSe, respectively.

Fig. 6 represents the heat capacity (C_V) as a function of temperature of the ternary alloys using GGA approach. It is obvious that at low temperature, C_V is proportional to T^3 [60], From 0 to about 400 K, C_V increases exponentially and then at high temperature (T > 400 K), the constant volume heat capacity C_V tends to the Dulong-Petit limit [61] (49.87 J/mol·K^{-1}) for the parent compounds CdSe and MgSe. In addition, C_V tends to the Dulong-Petit limit (197.47 J/mol·K^{-1}) for $Mg_xCd_{1-x}Se$ alloys (x = 0.25, 0.5 and 0.75). The temperature effect on bulk modulus (B) is given in Fig. 7 and it can be seen that B of $Cd_{1-x}Mg_xSe$ alloys decreases as temperature increases because the cell volume rapidly changes when the temperature is increased. A third-order polynomial fitting of B-T data at zero pressure is given as:

$$MgSe \rightarrow B(T) = 68.37 + 0.0016T - 5.86T^2 + 2.95T^3 \quad (21)$$

(P = 0) for T < 1000 K

$$CdSe \rightarrow B(T) = 60.07 - 0.035T - 3.58T^2 + 1.85T^3 \quad (22)$$

(P = 0) for T < 1000 K

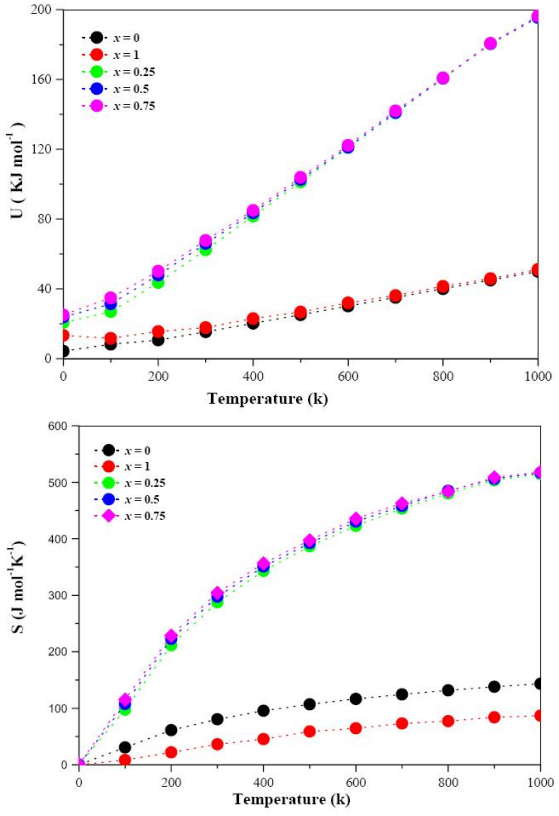

Fig. 5. Variation of the entropy (S) and the internal energy (U) versus temperature (T) of the $Mg_xCd_{1-x}Se$ alloys at different compositions x.

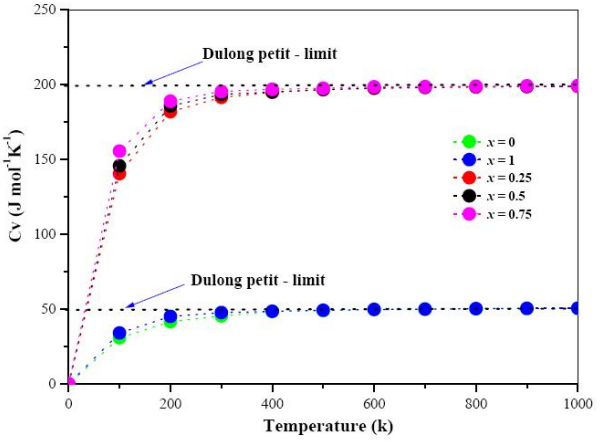

Fig. 6. Variation of the heat capacities C_V versus temperature T for $Mg_xCd_{1-x}Se$ alloys.

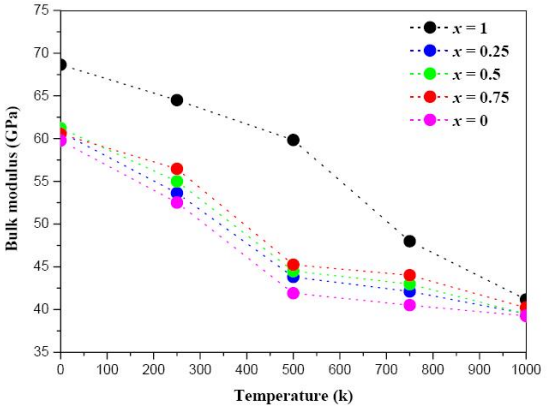

Fig. 7. Variation of bulk modulus versus temperature T for $Mg_xCd_{1-x}Se$ alloys.

At zero pressure and T = 300 K, the bulk modulus is equal to 50.29 and 62.57 GPa for the parent compounds CdSe and MgSe.

4. Conclusions

Density functional calculations have been carried out for the first time to investigate structural and optoelectronic properties of $Mg_xCd_{1-x}Se$. Structure as well as bonding nature of the material significantly varies with Mg concentration. The lattice parameter at different compositions is found to vary almost linearly, thus, obeying Vegard's law. The calculated band structures predicts that the alloys have direct band gap, which increases with the increase in x. On the basis of the wide range of fundamental direct band gaps (0.43 to 2.46 eV) and indirect band gaps (1.65 to 2.50 eV) between x = 0.25 and x = 0.75, it can be concluded that the material can be used in optoelectronic devices working in the IR and visible regions of spectrum. Also, the thermal effect on heat capacities has been investigated using the quasi-harmonic Debye model. To the best of the author's knowledge, no experimental values of the thermodynamic functions of the parent compounds CdSe and MgSe are found.

Acknowledgements

Y.A. would like to acknowlegde University Malaysia Perlis for Grant No. 9007-00111 and TWAS-Italy for the full support of his visit to JUST-Jordan under TWAS-UNESCO Associateship.

References

[1] PHILLIPS M.C., WANG M.W., SWENBERG J.F., MCCALDIN J.O., MCGILL T.C., *Appl. Phys. Lett.*, 61 (1992), 1962.

[2] JOBST B., HOMMEL D., LUNZ U., GERHARD T., LANDWEHR G., *Appl. Phys. Lett.*, 69 (1996), 97.

[3] FERREIRA S.O., SITTER H., KRUMP R., FASCHINGER W., BRUNTHALER G., SADOWSKI J.T., *Semicond. Sci. Tech.*, 10 (1995), 489.

[4] GAINES J.M., DRENTEN R.R., HABERERN K.W., MARSHALL T., MENSZ P., PETRUZZELLO J., *Appl. Phys. Lett.*, 62 (1993), 2462.

[5] SPIEGEL R., BACHER G., HERZ K., FORCHEL A., LITZ T., WAAG A., LANDWEHR G., *Phys. Rev. B*, 53 (1996), 4544.

[6] OH E., PARKS C., MIOTKOWSKI I., SCIACCA D.M., MAYUR A.J., RAMDAS A.K., *Phys. Rev. B*, 48 (1993), 15040.

[7] JOBST B., HOMMEL D., LUNZ U., GERHARD T., LANDWEHR G., *Appl. Phys. Lett.*, 69 (1996), 97.

[8] WANG M.W., PHILLIPS M.C., SWENBERG J.F., YU E.T., MCCALDIN J.O., MCGILL T.C., *J. Appl. Phys.*, 73 (1993), 4660.

[9] SAVRASOV S., SAVRASOV D., *Phys. Rev. B*, 46 (1992), 12181.

[10] SAVRASOV S.Y., *Phys. Rev. B*, 54 (1996), 16470.

[11] HOHENBERG P., KOHN W., *Phys. Rev. B*, 136 (1964), 864.

[12] KOHN W., SHAM L.J., *Phys. Rev. A*, 140 (1965), 1133.

[13] SAVRASOV S.Y., *Z. Kristallogr.*, 220 (2005), 555.

[14] PERDEW J.P., WANG Y., *Phys. Rev. B*, 46 (1992), 12947.

[15] BLOCHL P., JEPSEN O., ANDERSEN O.K., *Phys. Rev. B*, 49 (1994), 16223.

[16] MURNAGHAN F.D., *Proc. Natl. Acad. Sci. USA*, 30 (1944), 244.

[17] DISMUCKES J.P., EKSTROM L., POFF R.J., *J. Phys. Chem.*, 68 (1964), 3021.

[18] EL HAJ HASSAN F., AKDARZADEH H., *Mater. Sci. Eng. B*, 121 (2005), 170.

[19] CHARIFI Z., BAAZIZ H., EL HAJ HASSAN F., BOUARISSA N., *J. Phys.-Condens. Mat.*, 17 (2005), 4083.

[20] VEGARD L., *Z. Phys.*, 5 (1921), 17.

[21] JOBST B., HOMMEL D., LUNZ U., GERHARD T., LANDWEHR G., *Appl. Phys. Lett.*, 69 (1996), 97.

[22] EL HAJ HASSAN F., *Phys. Status Solidi B*, 242 (2005), 909.

[23] ZAKHAROV O., RUBIO A., BLASE X., COHEN M.L., LOUIE S.G., *Phys. Rev. B*, 50 (1994), 10780.

[24] HEYD J., PERALTA J.E., SCUSERIA G.E., MARTIN R.L., *J. Chem. Phys.*, 123 (17) (2005), 174101.

[25] YU P.Y., CARDONA M., *Fundamentals of Semiconductors*, Springer, Berlin, 2001.

[26] CHANG Y.H., PARK C.H., *J. Korean Phys. Soc.*, 49 (2006), 485.

[27] OKUYAMA H., NAKANO K., MIYAJIMA T., AKIMATO K., *J. Cryst. Growth*, 117 (1992), 139.

[28] KALPANA G., PALANIVEL B., THOMAS R.M., RAJAGOPALAN M., *Physica B*, 222 (1996), 223.

[29] RACHED D., BENKHETTOU N., SOUDINI B., ABBAR B., SEKKAL N., DRIZ M., *Phys. Status Solidi B*, 240 (2003), 565.

[30] DRIEF F., TADJER A., MESRI D., AOURAG H., *Catal. Today*, 89 (2004), 343.

[31] DUMAN S., BAĞCIS., TUTUNCU H.M., SRIVASTAVA G.P., *Phys. Rev. B*, 73 (2006), 205201.

[32] SAIB S., BOUARISSA N., RODRÍGUEZ-HERNÁNDEZ P., MUÑOZ A., *Eur. Phys. J. B*, 73 (2010), 185.

[33] WU Z., COHEN R.E., *Phys. Rev. B*, 37 (2006), 235116.

[34] DUAN Y., SHI H., QIN L., *Phys. Lett. A*, 372 (2008), 2930.

[35] DUAN Y., LI J., LI SH.-SH., XIA J.-B., *J. Appl. Phys.*, 103 (2008), 023705.

[36] MAQBOOL M., AMIN B., AHMAD I., *J. Opt. Soc. Am. B*, 26 (2009), 2180.

[37] DERKOWSKA B., FIRSZT F., SAHRAOUI B., MARASEK A., KUJAWA M., *Opto-Electron. Rev.*, 16 (1) (2008), 8.

[38] TSIDILKOVSKI I.M., *Band Structure of Semiconductors*, Elsevier Science & Technology Books, Amsterdam, 1982.

[39] ADACHI S., *Properties of Semiconductor Alloys: Group – IV, III – V and II – VI Semiconductors*, John Wiley & Sons Ltd., 2009.

[40] SALCEDO-REYES J.C., *Universitas Scientiarum*, 13 (2) (2008), 198.

[41] FIRSZT F., ŁĘGOWSKI S., MĘCZYŃSKA H., SEKULSKA B., SZATKOWSKI J., ZAKRZEWSKI J., PASZKOWICZ W., *Acta Phys. Pol. A*, 95 (6) (1999), 991.

[42] HERNÁNDEZ.CALDERÓN I., *Optical properties and electronic structure of wide band gap II – VI semiconductors*, in TAMARGO M.C., *II – VI Semiconductor Materials and their Applications*, Taylor and Francis, New York, 2002, 113.

[43] OKUYAMA H., KISHITA Y., ISHIBASHI A., *Phys. Rev. B*, 57 (1998), 2257.

[44] GÖKOĞLU G., DURANDURDU M., GÜLSEREN O., *Comp. Mater. Sci.*, 47 (2) (2009), 593.

[45] BERNARD J.E., ZUNGER A., *Phys. Rev. Lett.*, 34 (1986), 5992.

[46] WEI S.-H., FERREIRA L.G., BERNARD J.E., ZUNGER A., *Phys. Rev. B*, 42 (1990), 9622.

[47] KAYGORODOV V.A., SEDOVA I.V., SOROKIN S.V., SITNIKOVA A.A., NEKRUTKINA O.V., SHUBINA T.V., TOROPOV A.A., SOROKIN V.S., IVANOV S.V., *Phys. Status Solidi B*, 19 (2002), 229.

[48] HAMIZI N.A., JOHAN M.R., *Int. J. Electrochem. Sc.*, 7 (2012), 8458.

[49] REDDY R.R., *Defence Sci. J.*, 53 (3) (2003), 239.

[50] SINGH J., *Physics of Semiconductors and their Heterostructures*, McGraw-Hill, 1993, 84.

[51] BIENIEWSKI T.M., CZYZAK S.J., *J. Opt. Soc. Am.*, 53 (1963), 496.

[52] HUANG M.Z., CHING W.Y., *Phys. Rev. B*, 47 (1993), 9449.

[53] KOOTSTRA F., DE BOEIJ P.L., SNIJDERS J.G., *Phys. Rev. B*, 62 (2000), 7071.
[54] SZYBOWICZ M., KOZIELSKI M., FIRSZT F., LEGOWSKI S., MECZYNSKA H., SZATKOWSKI J., PASZKOWICZ W., *Opto-Electron. Rev.*, 7 (2) (1999), 103.
[55] BLANCO M.A., FRANCISCO E., LUNANA V., *Comput. Phys. Commun.*, 158 (2004), 57.
[56] PENG F., FU H.Z., CHENG X.L., *Physica B*, 400 (2007), 83.
[57] PENG F., FU H.Z., YANG X.D., *Solid State Commun.*, 145 (2008), 91.
[58] PENG F., FU H.Z., YANG X.D., *Physica B*, 403 (2008), 2851.
[59] BLANCO M.A., PENDAS A.M., FRANCISCO E., RECIO J.M., FRANKO R., *J. Mol. Struct.*, 368 (1996), 245.
[60] DEBYE P., *Ann. Phys.-Berlin*, 344 (14) (1912), 789.
[61] PETIT A.T., DULONG P.L., *Ann. Chim. Phys.*, 10 (1819), 395.

Received 2014-07-21
Accepted 2014-09-24